



Transcriptional Response of *Wolbachia* to Dengue Virus Infection in Cells of the Mosquito *Aedes aegypti*

 Michael Leitner,^a Cameron Bishop,^a  Sassan Asgari^a

^aAustralian Infectious Disease Research Centre, School of Biological Sciences, The University of Queensland, Brisbane, Australia

ABSTRACT *Aedes aegypti* transmits one of the most significant mosquito-borne viruses, dengue virus (DENV). The absence of effective vaccines and clinical treatments and the emergence of insecticide resistance in *A. aegypti* necessitate novel vector control strategies. A new approach uses the endosymbiotic bacterium *Wolbachia pipientis* to reduce the spread of arboviruses. However, the *Wolbachia*-mediated antiviral mechanism is not well understood. To shed light on this mechanism, we investigated an unexplored aspect of *Wolbachia*-virus-mosquito interaction. We used RNA sequencing to examine the transcriptional response of *Wolbachia* to DENV infection in *A. aegypti* Aag2 cells transfected with the wAlbB strain of *Wolbachia*. Our results suggest that genes encoding an endoribonuclease (RNase HI), a regulator of sigma 70-dependent gene transcription (6S RNA), essential cellular, transmembrane, and stress response functions and primary type I and IV secretion systems were upregulated, while a number of transport and binding proteins of *Wolbachia*, ribosome structure, and elongation factor-associated genes were downregulated due to DENV infection. Furthermore, bacterial retrotransposon, transposable, and phage-related elements were found among the up- and downregulated genes. We show that *Wolbachia* elicits a transcriptional response to virus infection and identify differentially expressed *Wolbachia* genes mostly at the early stages of virus infection. These findings highlight *Wolbachia*'s ability to alter its gene expression in response to DENV infection of the host cell.

IMPORTANCE *Aedes aegypti* is a vector of several pathogenic viruses, including dengue, Zika, chikungunya, and yellow fever viruses, which are of importance to human health. *Wolbachia* is an endosymbiotic bacterium currently used in transinfected mosquitoes to suppress replication and transmission of dengue viruses. However, the mechanism of *Wolbachia*-mediated virus inhibition is not fully understood. While several studies have shown mosquitoes' transcriptional responses to dengue virus infection, none have investigated these responses in *Wolbachia*, which may provide clues to the inhibition mechanism. Our results suggest changes in the expression of a number of functionally important *Wolbachia* genes upon dengue virus infection, including those involved in stress responses, providing insights into the endosymbiont's reaction to virus infection.

KEYWORDS *Aedes aegypti*, wAlbB, *Wolbachia*, dengue virus, mosquito, transcription

Arthropod-borne viruses (arboviruses) account for a significant number of viral infections in humans and livestock, representing a considerable global public health burden (1, 2). Dengue virus (DENV) is overwhelmingly the most important mosquito-borne flavivirus, responsible for an estimated 390 million infections annually with a further 2.5 billion people at risk of infection worldwide (1, 3). DENV consists of four distinct serotypes (DENV-1 to -4) and is a member of the *Flaviviridae* family that encompasses lipid-enveloped, single-stranded positive-sense RNA viruses (4). The main transmission vectors, the mosquitoes *Aedes aegypti* and *Aedes albopictus*, are

Citation Leitner M, Bishop C, Asgari S. 2021. Transcriptional response of *Wolbachia* to dengue virus infection in cells of the mosquito *Aedes aegypti*. *mSphere* 6:e00433-21. <https://doi.org/10.1128/mSphere.00433-21>.

Editor Barbara J. Campbell, Clemson University

Copyright © 2021 Leitner et al. This is an open-access article distributed under the terms of the [Creative Commons Attribution 4.0 International license](https://creativecommons.org/licenses/by/4.0/).

Address correspondence to Sassan Asgari, s.asgari@uq.edu.au.

Received 6 May 2021

Accepted 7 June 2021

Published 30 June 2021

distributed in high abundance worldwide, especially in regions with tropical and subtropical climates such as Asia, mid-Africa, Central America, and most of South America (5, 6). DENV has fully adapted to a human-mosquito-human transmission cycle, with *A. aegypti* being the primary vector of DENV in high-density urban environments (7, 8). *A. albopictus* is also capable of transmitting DENV; however, it predominantly colonizes suburban, rural, and forest areas (8). Dramatic increases in population density accompanied by rapid urbanization and cross-linked global transport systems are responsible for the rise of mosquito vectors throughout the tropical regions of the world (1, 7–9).

In light of the absence of an effective vaccine or clinical treatment, sustainable alternatives to control the global spread of DENV are being investigated. Historically, vector control programs against *A. aegypti*, reliant on chemical and biological agents, have been the methods of choice to reduce DENV transmissions (10). However, with the emergence of insecticide resistance in *A. aegypti* across many regions of the world, the effectiveness of chemical-based vector control interventions has declined dramatically (10–13). As a result, novel vector control strategies are needed to stop the expansion of mosquito-borne arboviruses.

A new effective approach to reduce the spread of arboviruses such as DENV, Zika virus (ZIKV), and chikungunya virus (CHIKV) uses the endosymbiotic bacterium *Wolbachia pipientis* as a biological control agent (14–16). It is estimated that various strains of *Wolbachia* infect 40% to 60% of all arthropod species (17–19). *Wolbachia* are Gram-negative, obligate intracellular alphaproteobacteria that have evolved to invade, influence, and manipulate their arthropod host's reproductive system in order to establish within a host population (18, 20, 21). *Wolbachia*'s ability to proliferate through a population is mainly achieved by inducing cytoplasmic incompatibility (CI) in its host (20, 22). The phenomenon of CI occurs when a *Wolbachia*-infected male insect mates with a female insect that is uninfected or not infected with a compatible strain of *Wolbachia*, generating nonviable offspring (20, 22). Consequently, CI promotes the unaided dispersion of the exclusively maternally inherited *Wolbachia* infection into the host population (20, 22). Additionally, in *Wolbachia*-transinfected female mosquitoes, *Wolbachia* conveys a fitness advantage by protecting the mosquitoes against infectious microbes, including viruses (20, 23, 24). The ability of certain strains of *Wolbachia* to provide protection against RNA virus infections was originally discovered in *Drosophila melanogaster* by two independent groups of researchers in 2008 (25, 26). The discovery of this insect protection against RNA viruses revealed the association between virus resistance and *Wolbachia* infection, paving the way for an effective mechanism to control mosquito-borne diseases.

Wolbachia does not naturally occur in *A. aegypti*; however, stable transfections can be achieved through microinjections (27). Several studies in *A. aegypti* investigating artificially introduced *Wolbachia* strains such as *wMelPop*, *wMel*, and *wAlbB* have demonstrated *Wolbachia*-induced changes in expression of immune-related genes (15, 28, 29). These findings led the way to two main hypotheses for *Wolbachia*-mediated virus inhibition, that of host innate immune priming and the competition for limited cellular host resources required for virus replication (14, 30). Mosquito species such as *A. aegypti* depend on their innate immune system to control arbovirus replication, as they lack the adaptive immune system of vertebrates (31). The interaction between the replicating DENV and its host *A. aegypti*'s innate immune system affects viral replication and the successive transmission of DENV (32). In this regard, a number of studies have found that the innate immune response and mediated pathways such as the RNA interference (RNAi), Toll, immune deficiency (IMD), and JAK/STAT signaling pathways have antiviral effects in *A. aegypti* (33, 34). Initially, the innate immune response in mosquitoes is activated through the recognition of pathogens by various receptors (35). The RNAi pathway is activated by the detection of double-stranded RNA (dsRNA) molecules of viral genomes or replication intermediates (34). Within the RNAi pathway, two RNA molecules, microRNA (miRNA) and small interfering RNA (siRNA), are vital for the RNAi pathway's functionality (36). Interestingly, both miRNAs and siRNAs are

modified upon *Wolbachia* infections (37). The inhibition of certain miRNAs induces a reduction of *Wolbachia* density, indicating that *Wolbachia* promotes its own preservation within the host (37). Several studies have confirmed that *Wolbachia* infections enhance the basal gene expression of the Toll, JAK/STAT, and RNAi pathways (15, 28, 29, 38). A study conducted in an *A. aegypti* (Aag2)-derived clonal cell line infected with *Wolbachia* demonstrated upregulation of endonuclease argonaute-2 (Ago2), a core catalytic component within the RNA-induced silencing complex (RISC) of the RNAi pathway (38). The *Wolbachia*-induced upregulation of Ago2 results in increased activity of the RNAi pathway, subsequently providing better protection against arboviruses (38). Overall, these findings have identified the RNAi pathway as the key insect antiviral pathway capable of limiting arboviruses such as DENV, CHIKV, and Sindbis virus (SINV) (31, 32, 39). However, studies suggest that RNAi may play no or a limited role in *Wolbachia*-mediated virus inhibition (38, 40).

Competition for limited cellular host resources also has been subject to investigations (14, 41). In particular, blood meal-derived molecules such as cholesterol are essential in mosquito egg development (41, 42). *A. aegypti* infected with *Wolbachia* strains *wMelPop* and *wMel* showed a 15% to 25% reduction in total cholesterol quantities compared to that in uninfected controls (41). However, subsequent cholesterol supplementation administered via blood meal did not correct the altered embryo morphology phenotype, and it did not improve fecundity or egg viability deficits (41). Understanding the contributions of *A. aegypti*, DENV, and *Wolbachia* in the virus inhibition phenotype is challenging and is further complicated by the fact that *Wolbachia* cannot be genetically modified (30, 43). The majority of knowledge to date has been gained from comparing the durability and level of *Wolbachia*-mediated virus inhibition in different combinations of vector species, virus genotypes, and *Wolbachia* strains (30, 44). Dissecting the mechanism of *Wolbachia*-mediated virus inhibition in *A. aegypti* proves difficult, and the inhibition is likely multilayered, with no individual mechanism responsible for this phenotype (30, 43). The diverse differences of *Wolbachia* strains infecting the same *A. aegypti* host confirm the contribution of the symbiont's genome to the mosquito-*Wolbachia* association (30, 45). Remarkably, the ability and magnitude of *Wolbachia*-mediated antiviral inhibition can differ between *Wolbachia* strains (15, 46–50).

Thus far, the arthropod host *A. aegypti* response to viral infections has been extensively investigated; however, to our knowledge, the transcriptional response of *Wolbachia* to virus infections in the mosquito has not. For this reason, we examined whether *Wolbachia*'s transcriptional response to DENV infection may shed light on the *Wolbachia*-mediated viral inhibition mechanism based on the function of differentially expressed genes. To test our hypothesis, we compared the transcriptional response of *Wolbachia wAlbB* strain to DENV infection in a transinfected *A. aegypti* (Aag2)-derived cell line. The outcomes of this study provide a basis for follow-up investigations into the mechanism.

RESULTS

RNA-Seq data analysis of Aag2.wAlbB cells after infection with DENV. To identify differentially expressed genes of *Wolbachia wAlbB* strain in response to DENV infection in transinfected *A. aegypti* Aag2 cells, DENV-2-infected and uninfected Aag2.wAlbB cells were collected at 1, 6, and 24 h postinfection (hpi) in three biological replicates for each time point. We chose these early time points, because previous studies have indicated that *Wolbachia*-mediated virus inhibition is exerted at early hours of infection in insect cells, including mosquito cells (51, 52). Prior to the experiment, *wAlbB*'s relative density was quantified by quantitative PCR (qPCR), which showed amplification of the *wsp* gene in Aag2.wAlbB cells, whereas no amplification of the gene was detected in the Aag2.tet cells (Aag2.wAlbB cells previously treated with tetracycline to remove *Wolbachia*) (Fig. 1A). *Wolbachia* density is expressed in terms of the number of *wsp* copies relative to the number of the mosquito's *RPS17* copies. Furthermore, increasing

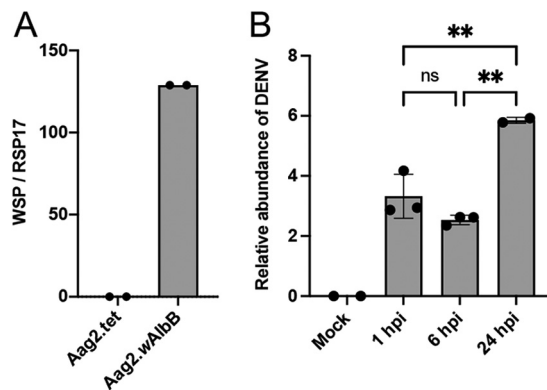


FIG 1 Relative density of *Wolbachia* in Aag2.wAlbB cell line and infectivity of the DENV inoculum. (A) The relative *Wolbachia* density was measured by qPCR analysis using genomic DNA extracted from Aag2.wAlbB cells and tetracycline-cured *Wolbachia*-free Aag2.tet cells as a control. Primers targeting the *Wolbachia* surface protein gene (*wsp*) and *A. aegypti* *RPS17* to amplify the target and normalizing genes were used, respectively. (B) Validation of virus infection by RT-qPCR analysis confirming DENV-2 genome copy accumulation in infected Aag2.wAlbB samples used for RNA-Seq. Uninfected Aag2.wAlbB cells served as control (mock). Sample 24a-infected was excluded from analysis. The bars and error bars represent means and standard deviations (SDs), respectively, from the three biological replicates. One-way analysis of variance (ANOVA) with Tukey's *post hoc* multiple-comparison tests were used for data analysis. ns, not significant; **, $P < 0.01$.

DENV genome copy accumulation was confirmed in the samples at time points 1, 6, and 24 hpi by quantitative reverse transcription-PCR (RT-qPCR) (Fig. 1B). While DENV genome copy numbers did not significantly change between 1 and 6 hpi, a significant increase in genome copy numbers was detected at 24 hpi. Based on a previous study in *A. albopictus* C6/36 cells, accumulation of viral genomic RNA of the four DENV serotypes started from 13 to 18 hpi (53). Therefore, no detectable viral replication between 1 and 6 hpi is expected.

Illumina HiSeq sequencing of RNA from DENV-2-infected and uninfected Aag2.wAlbB cells generated a total of 1,629,779,502 raw reads with 150-bp paired-ends from the 18 RNA samples (see Table S2 in the supplemental material). Following the adapter trimming and quality filtering using the trim reads sequence tool in CLC Genomics Workbench (CLC-GWB), a total of 1,629,758,722 high-quality reads remained. Each sample and each biological condition were represented by an average of 92,742,982 and 88,341,320 million reads, respectively. The trimmed reads with a Phred quality score of $>Q30$ corresponding to an error rate of 0.04% were mapped to the *A. aegypti* three chromosomes, mitochondrion, wAlbB, DENV-2, and Aag2 cell line-related viruses (cell-fusing agent virus [CFAV] and *Aedes albopictus* negev-like virus [AaNLV]) reference genomes using the RNA sequencing (RNA-Seq) analysis tool in CLC-GWB as described in Materials and Methods. An average of 90,044,894 and 86,018,515 reads mapped to the *A. aegypti*, wAlbB, and virus genomes in the DENV-infected and uninfected samples, respectively, equivalent to 97.4% of the total reads (Fig. 2). Sample 24a infected with DENV-2 was excluded from further analysis, as we found that RNA from Aag2.tet cells at 24 hpi was accidentally submitted for sequencing instead of Aag2.wAlbB at 24 hpi. However, the data were used for *de novo* assembly of the DENV-2 ET-300 genome (see below). For each sample and biological condition, averages of 27,005,569 and 29,785,073 reads for DENV-infected and uninfected samples, respectively, equivalent to 29.1% to 33.7%, were mapped to the wAlbB's reference genome (54). Principal-component analysis (PCA) analysis showed distinct separation at 1, 6, and 24 hpi between DENV-infected and uninfected Aag2.wAlbB samples, indicating a high level of similarity among the biological replicates from different samples (Fig. 3). The 2.6% unmapped reads were used for *de novo* assembly of contigs using the CLC-GWB *de novo* assembly tool. BLASTn analysis of the assembled contigs to the nonredundant nucleotide NCBI DNA database produced a variety of long and short contigs. The longest contigs

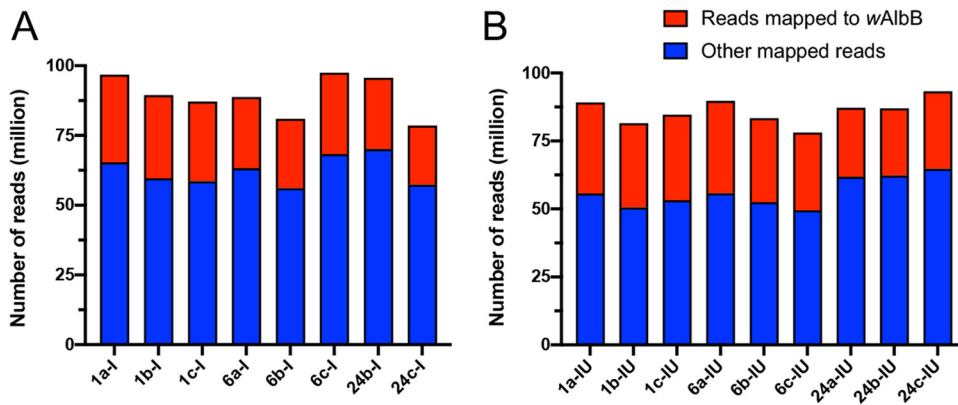


FIG 2 Composition of Aag2.wAlbB normalized reads mapped to the combined reference file and the wAlbB reference genome. Aag2.wAlbB reads were mapped to *A. aegypti*, wAlbB, and viral reference genomes for DENV-infected (A) and uninfected (B) Aag2.wAlbB cells. Sample 24a-infected was excluded from analysis. The bars represent total numbers of reads mapped to all the genomes, with the red portion representing reads mapped to the wAlbB genome and the blue portion representing reads that did not map to the wAlbB genome but to the rest (*A. aegypti* and viral reference genomes).

between 1,801 and 13,186 bp in size were identified as additional *A. aegypti* host-related viruses, Aedes anphevirus, Primus virus, Phasi Charoen-like virus, Aedes albopictus densovirus, Australian Anopheles totivirus, and unplaced scaffolds of *A. aegypti* genome artifacts (55).

Full-length virus genome read counts expressed in normalized read counts (trimmed mean of M values [TMM] adjusted) confirmed the increasing DENV abundance in each DENV-infected Aag2.wAlbB sample used for RNA-Seq (Fig. 4).

Transcriptional response by *Wolbachia* with respect to time and DENV infection.

A total of 96 genes were significantly differentially expressed across the three time points combined; 13, 31, and 52 differentially expressed genes (DEGs) at 1 versus 6, 6 versus 24, and 1 versus 24 hpi, respectively (Fig. 5; see also Table S3). There was a total of 16 DEGs that overlapped between the time points (Fig. 5). The open reading frames (ORFs) from the identified DEGs featured complete coding with no premature stop codon truncations. Approximately one-quarter of those DEGs, 26.0% (25), were upregulated versus 74.0% (56) being significantly downregulated. Specifically, 4, 13, and 8 genes were upregulated at 1 versus 6, 6 versus 24, and 1 versus 24 hpi in contrast to 9, 18, and 44 downregulated genes at the three time points, respectively (Table S3).

Among the upregulated genes at 1 versus 6 hpi were those encoding transposases, conjugal transfer protein TraJ from the type IV secretion system, and MSF transporter. Downregulated genes identified in that comparison were those encoding an ATPase, ankyrin repeat domain-containing protein, RNase HI, ATP synthase subunit C, and five hypothetical proteins (Table S3). DEGs, when 6 and 24 hpi samples were compared, represented transposases, ankyrin repeat domain-containing proteins, RuvC, *O*-methyltransferase, a number of ribosomal proteins, maturase, ferredoxin, MspII family outer membrane protein, elongation factor Tu, a reductase, TrbC from the type IV secretory system, iron-sulfur cluster assembly accessory protein, sodium:proton antiporter, and a number of hypothetical proteins (Table S3). When data from 1 versus 24 hpi were compared, similar types of genes were differentially expressed, including those encoding transposases, *O*-methyltransferase, maturase, epimerase, ribosomal proteins, ion antiporters, ATPases, elongation factor Tu, and ankyrin repeat domain-containing proteins plus a number of other proteins that are all listed in Table S3.

Transcriptional response by *Wolbachia* to DENV infection. When DENV-infected and uninfected samples at each time point were compared, a total of 22 genes were significantly differentially expressed across the three time points combined, considering a fold change of ≥ 2.0 and an adjusted *P* value of < 0.05 : 4, 5, and 13 DEGs at 1, 6, and 24 hpi, respectively (Fig. 6; see also Table S4). These included genes encoding DNA mismatch repair protein MutS, RNase HI, and transposases at 1 hpi, glutathione

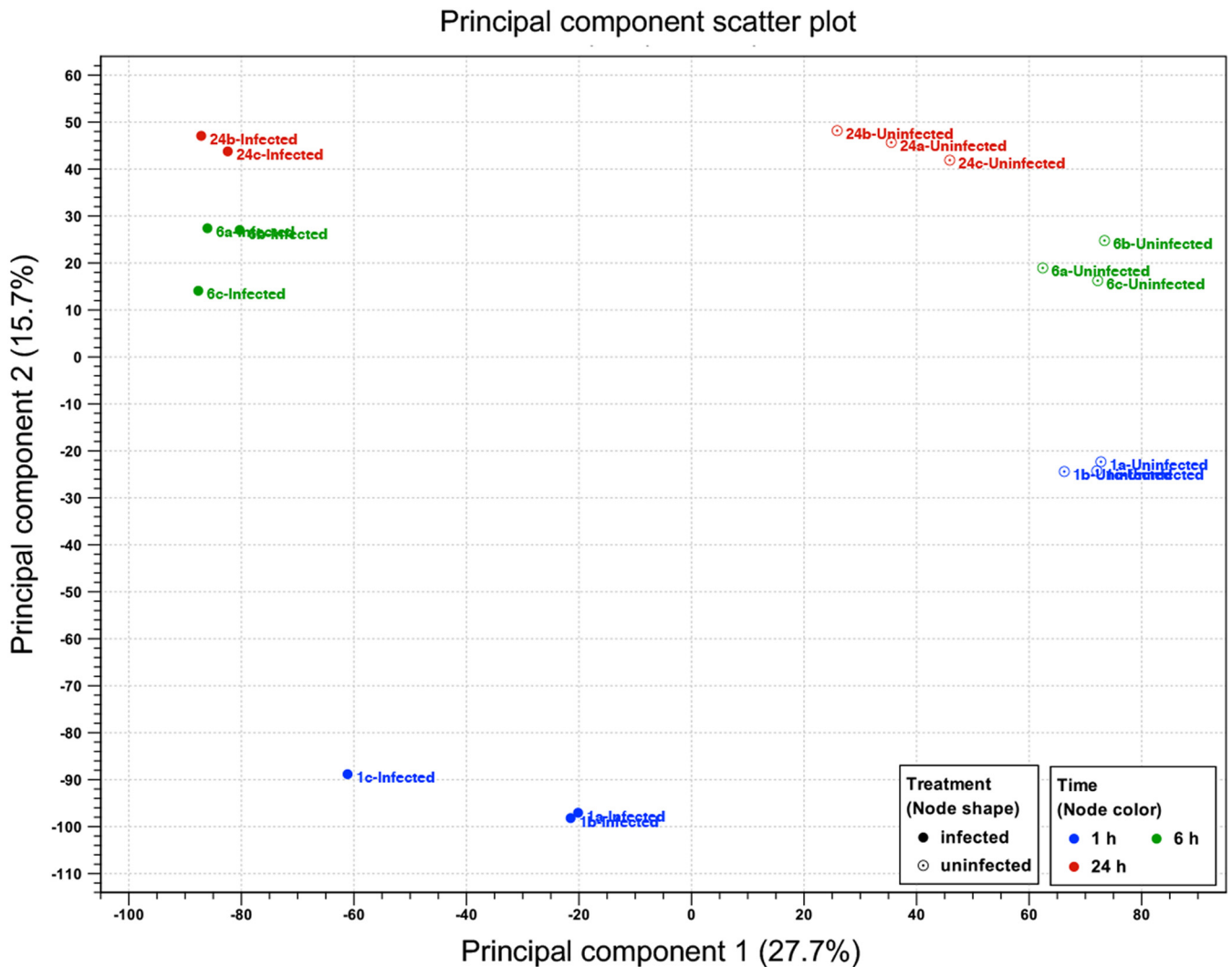


FIG 3 Principal-component analysis (PCA) of the RNA-Seq samples. The PCA figure represents a two-dimensional scatterplot of the first two principal components of the RNA-Seq data. DENV-infected and uninfected Aag2.wAlbB sample groups at different time points are represented by different colors as indicated by the legend provided within the graph. Each dot represents a biological replicate of an RNA-Seq sample. Sample 24a-infected was excluded from analysis.

synthase, group II intron reverse transcriptase, and transposase at 6 hpi and *O*-methyltransferase, SPFH domain-containing protein, group II intron reverse transcriptases, sodium:proton antiporter, ribosomal proteins, and iron-sulfur cluster assembly accessory protein at 24 hpi (Table S4). There was only one DEG that overlapped between the time points, encoding DNA mismatch repair protein MutS (Fig. 6).

However, considering a fold change of ≥ 1.5 , a total of 148 genes were significantly differentially expressed across the three time points combined: 39, 65, and 44 DEGs at 1, 6, and 24 hpi, respectively (Fig. S2; Table S4). There was a total of 11 overlapping DEGs between the time points (Fig. S2). These included genes encoding MutS, ATP-binding protein, DnaJ, two group II intron reverse transcriptases, ankyrin domain-containing protein, TatD hydrolase, cytidyltransferase, ribosomal protein S9, and a hypothetical protein. A third of those DEGs, 25.0% (37), were upregulated versus 75.0% (57) being significantly downregulated. Specifically, 21, 1, and 15 genes were upregulated at 1, 6, and 24 hpi in contrast to 18, 64, and 29 downregulated genes at the three time points, respectively (Table S4).

***De novo* assembly of DENV-2 ET-300 genome.** Despite the usage of DENV-2 ET-300 strain in several studies, the complete genome of the virus was not available on

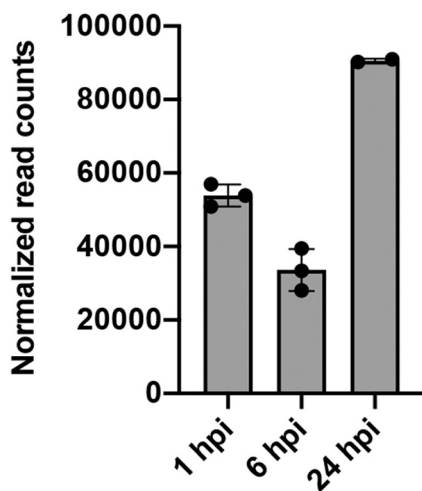


FIG 4 Accumulation of DENV-2 read counts following infection in RNA-Seq samples. Validation of virus infection: full-length virus genome read counts expressed in normalized read counts (TMM adjusted) confirmed DENV abundance in each infected Aag2.wAlbB sample used for RNA-Seq. Sample 24a-infected was excluded from analysis. The bars and error bars represent means and SDs from the three biological replicates.

GenBank at the time this study took place. To assemble the viral genome, we used reads from Aag2.wAlbB sample 24a. In Aag2.wAlbB sample 24a, 678,422 of 100,812,616 (0.67%) reads mapped to a 10,696-nucleotide long contig, achieving an average coverage of 9,476 \times . The largest ORF from this contig showed complete coding with no premature stop codon truncations present. The ORF is 10,176 nucleotides in length and encodes a 3,392-amino-acid polyprotein. BLASTn analysis identified the ORF as 99.28% identical with the highest pairwise nucleotide identity (10,091/10,164) to dengue virus 2 genomic RNA, strain D2/Hu/OPD030NIID/2005 (GenBank identifier [ID] [LC111438.1](#); E value, 0.0; query cover, 99%). BLASTp analysis of the ORF revealed that it is most similar to the polyprotein of dengue virus 2 (GenBank ID [BAU36333.1](#); E value, 0.0; identity, 99.71%; query cover, 100%) and contains the three classic structural (C, prM, and E) and seven nonstructural (NS1, NS2A, NS2B, NS3, NS4A, NS4B, and NS5) proteins of the DENV polyprotein (58–60). The complete genome sequence obtained in this study is

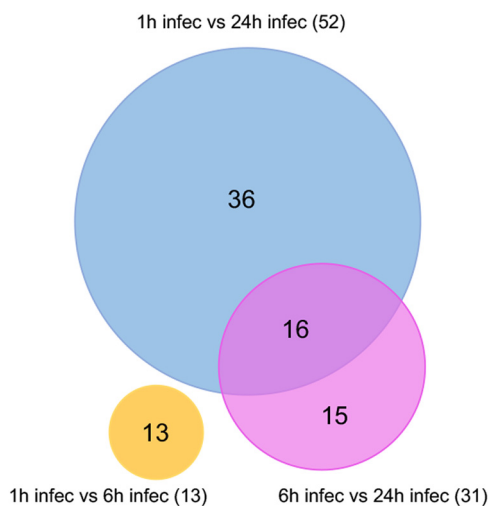


FIG 5 Differentially expressed genes in wAlbB across time points after DENV infection. Venn diagram showing DEGs (fold change of ≥ 2.0 and an adjusted *P* value of < 0.05) in wAlbB in DENV-infected Aag2.wAlbB mosquito cells when different time points were compared. Sixteen overlapping DEGs were found between the time points. Each colored circle represents a sample collection time point.

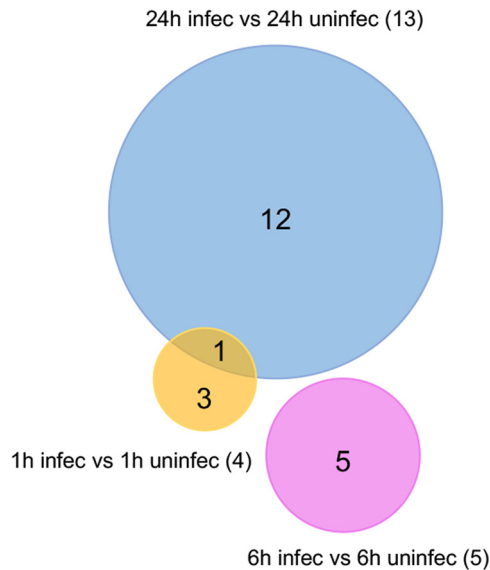


FIG 6 Differentially expressed genes in *wAlbB* due to DENV infection. Venn diagram showing DEGs (fold change of ≥ 2.0 and an adjusted P value of < 0.05) in *wAlbB* in DENV-infected versus uninfected Aag2.*wAlbB* mosquito cells at each time point. One overlap of DEGs was found between the time points. Each colored circle represents a sample collection time point.

100% identical to a recently deposited sequence for DENV-2 ET-300 (accession number [MT921572](#)).

Validation of DEGs by quantitative reverse transcription-PCR. The representative selection of differentially expressed *Wolbachia* genes identified by RNA-Seq analysis was validated by RT-qPCR. For this, the DENV infection experiment was repeated in Aag2.*wAlbB* cells with identical conditions to the preparation of samples for RNA-Seq. DENV infection was confirmed in cells collected at 1, 6, and 24 hpi (see Fig. S3). The results showed an overall consistency between RNA-Seq and RT-qPCR, when DEGs in DENV-infected Aag2.*wAlbB* cells with respect to time and DENV infection were considered (Fig. 7A). Similarly, we found consistency between the two approaches when DENV-infected and uninfected samples were compared (Fig. 7B).

DISCUSSION

The endosymbiotic bacterium *Wolbachia* has proven to be an effective biocontrol strategy to reduce the transmission of arboviruses by mosquitoes. A number of studies have confirmed that *Wolbachia* confers antiviral protection in primary arbovirus mosquito vectors (14–16, 61). Nonetheless, the mechanism underlying the *Wolbachia*-mediated viral protection is not yet well understood. The mosquito host *A. aegypti* response to viral infections has been extensively investigated (56, 62, 63); however, to our knowledge, the transcriptional response of *Wolbachia* to virus infections in the mosquito has not. For this reason, we examined whether *Wolbachia*'s transcriptional response to DENV infection could shed light on the *Wolbachia*-mediated viral inhibition mechanism based on the function of differentially expressed genes. We used RNA-Seq in order to study the transcriptional response of the *Wolbachia wAlbB* strain to DENV-2 infection in *A. aegypti* Aag2 cells.

We found an exponential increase of the transcriptional changes of *Wolbachia* with respect to time and DENV infection occurring between 1 and 6 hpi (13 DEGs), followed by 6 and 24 hpi (31 DEGs), with most changes between 1 and 24 hpi (52 DEGs). Similarly, the transcriptional response by *Wolbachia* to DENV infection when comparing DENV-infected versus uninfected Aag2.*wAlbB* cells at 1, 6, and 24 hpi showed increases in transcriptional changes across the three time points for 4, 5, and 13 genes, respectively. At 1 hpi, we identified a gene encoding an endoribonuclease (RNase HI)

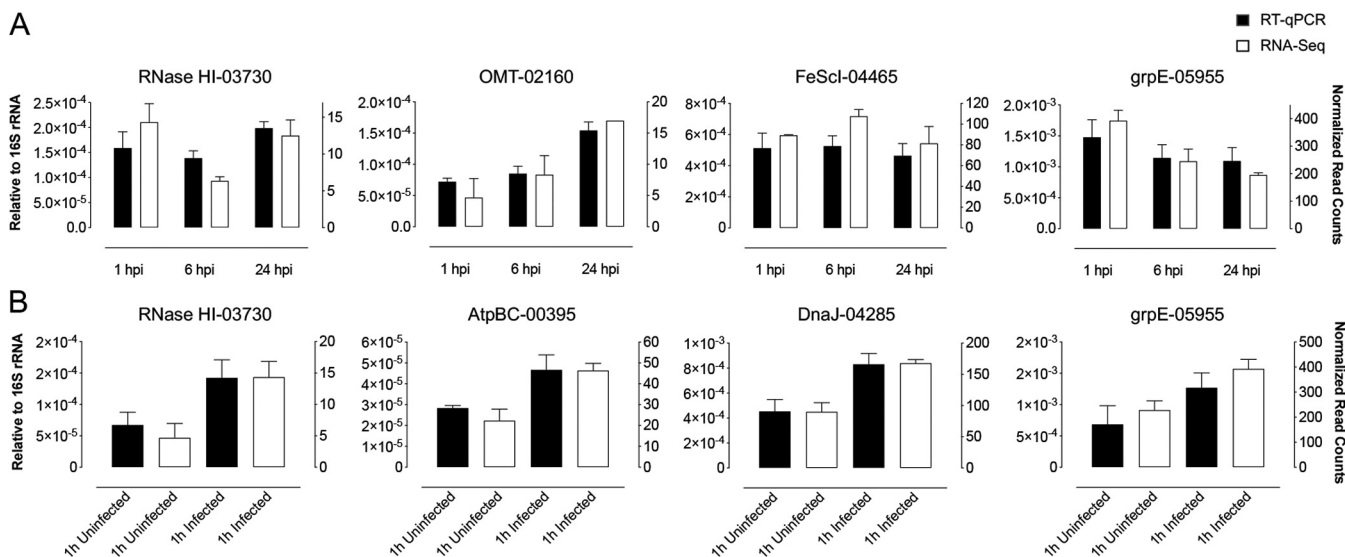


FIG 7 Validation of differentially expressed *Wolbachia* genes after DENV-2 infection using RT-qPCR. (A) The bar graphs represent RNA-Seq normalized gene reads and RT-qPCR relative expression results of the DEGs in DENV-infected Aag2.wAlbB cells with respect to time and DENV infection. (B) The bar graphs represent RNA-Seq normalized gene reads and RT-qPCR relative expression results of the DEGs in DENV-infected versus uninfected Aag2.wAlbB cells at 1 hpi.

as significantly upregulated due to DENV infection. RNase HI plays an essential role in bacterial cellular processes such as DNA replication, gene expression, DNA repair, and degradation of RNA (64–66) and is an endoribonuclease with the capability of degrading RNA/DNA hybrids generated during viral replication in a non-sequence-specific manner (64, 66, 67). Furthermore, studies have suggested that RNase HI could play a vital role in antiviral defense in prokaryotes (68–71).

Using a fold change difference of ≥ 1.5 provided a more complete insight into *Wolbachia*'s transcriptional response to DENV infection and uncovered a number of significant differentially expressed genes related to stress response, secretion, and fundamental bacterial cellular functions based on annotation. Among the upregulated genes at 1 hpi were genes encoding the DNA mismatch repair protein MutS, molecular chaperone DnaJ, nucleotide exchange factor GrpE, ATP-binding cassette (ABC) domain-containing protein, and type I (HlyD family periplasmic adaptor subunit) and IV (conjugative DNA transfer family protein VirD4 and P-type conjugative transfer protein VirB9) secretory system elements. *mutS* encodes an essential DNA mismatch repair protein, MutS, that identifies and corrects errors generated during DNA replication and other biological processes (72, 73). The heat shock molecular chaperone protein-encoding genes *dnaJ* and *grpE* participate in responses to heat shock and cellular stress, stabilizing proteins by preventing their denaturation and actively refolding denatured proteins (74–78). Both *dnaJ* and *grpE* are part of the major DnaK/DnaJ chaperone system used by prokaryotic symbionts in response to stress (78, 79). The nucleotide exchange factor GrpE functions as a molecular cochaperone promoting the exchange of ADP for ATP from DnaK within the bacterial cytoplasm (75, 76). ABC domain-containing proteins are part of the ABC transmembrane transport system involved in the import of essential nutrients and the export of various molecules such as proteins, lipids, and toxins (80–82). In *Wolbachia*, ABC transmembrane transporters are embedded in the inner membrane and usually connected to a membrane fusion protein that crosses the periplasmic space (83). The type I secretion system (T1SS) is a basic secretion system spanning both the inner and outer membranes of *Wolbachia* (83–85). This enables the transport of substrates (e.g., DNA and proteins) from the cytoplasm to outside the cell into the host (83–85). The T1SS is composed of three proteins: an ABC transporter/ATPase (ABC) embedded in the inner membrane, a membrane

fusion protein, and an outer membrane protein (83, 85). The T4SS protein VirD4 is an important ATPase known as a coupling protein responsible for substrate recruitment within the T4SS (86, 87). The T4SS transports substrates (e.g., DNA and proteins) from the cytoplasm to outside the cell or into various target recipients, including eukaryotic cells, and spans both membranes and the periplasm (83, 87–89). Essentially, all members of the *Rickettsiales* harbor T1SS and T4SS implicated in their establishment, pathogenicity, and transmission (83). Despite all of these genes being significantly upregulated or induced at the very early time point of DENV infection, they were all downregulated over time, i.e., at 24 hpi.

Among the downregulated genes at 1 hpi is an RNase (RNAP), a DNA-dependent RNA polymerase known as the key enzyme in gene expression and regulation in bacteria (90–92). Despite the fact that the gene encoding the RNA polymerase was downregulated at 1 hpi, it was upregulated over time, and the mean gene expression across all biological replicates and time points remained very high. Furthermore, two ankyrin repeat-containing (ANK) proteins and a site-specific recombinase were identified as WO prophage-related genes (54, 93, 94). ANK (DEJ70_02765) and the site-specific recombinase (DEJ70_04945) are located within the *wAlbB* WO-like island 01 and *wAlbB* WO-like island 02, respectively. ANK proteins are rare in most bacteria; however, 34 *wAlbB* proteins contain at the minimum one copy of an ANK repeat domain, with a total of 81 copies of various types of ANK repeat domains (54). More than 30 *Wolbachia* strains from different insect and nematode hosts feature these ANK repeat regions (83, 94–96). These ANK proteins mediate a wide range of protein-protein interactions, such as transcription initiation and signaling, and are believed to be involved in *Wolbachia*-host interactions (54, 94–97).

At 6 hpi, a regulator of sigma 70-dependent gene transcription *ssrS* (6S RNA), a highly abundant noncoding RNA (ncRNA), was the only DEG upregulated, whereas all 64 of the other DEGs were downregulated (98–102). Concurrently, DENV genome copy numbers decreased notably at 6 hpi. Studies in *Escherichia coli* and other bacteria have shown that 6S RNA specifically binds σ 70 RNA polymerase capable of inhibiting and downregulating transcription at σ 70-dependent promoters (98–102). Furthermore, ncRNAs such as 6S RNA have been identified to perform several essential functions such as RNA processing, gene regulation, and interaction with proteins in addition to mRNAs (57, 98–102). In *Wolbachia* strains, *wMel*, *wMelPop-CLA*, *wMelCS*, and *wAu* studies discovered a range of ncRNAs and confirmed their biological functionality (57, 103). However, both studies failed to detect 6S RNA in the *Wolbachia* strains used. Mayoral et al. used Illumina TruSeq small RNA deep sequencing and detecting read fragments of 40 bp in size (103), whereas Woolfit et al. produced sequence fragments of 300 bp, acknowledging that this size is longer than most known small RNAs (sRNAs) (57). Eminently, 6S RNA in *wAlbB* is 162 bp in size, containing conserved prokaryotic promoter regions and boxes –35 and –10 indicative of its functionality to regulate bacterial and even host gene transcription, as previously described (103).

At the later time point, 24 hpi, the majority of DEGs were related to ribosomal structure, translation, DNA mismatch repair, transmembrane, and stress response. Furthermore, a number of secretion system subunit-encoding genes were downregulated due to DENV infection over time. Bacterial transposable elements and a number of hypothetical proteins were found among the upregulated and downregulated genes across all time points. IS3, and IS66 family transposase are insertion sequences (IS) which comprise the simplest form of transposable elements (TEs) of a transposase gene, flanked by inverted repeats (54, 104, 105). IS elements comprise 13% of the *wAlbB* genome, corresponding to a total number of 218 different IS element families (54).

Furthermore, 16 overlapping DEGs were identified between 6- and 24-hpi and 1- and 24-hpi time points. Most of these genes are related to basic bacterial cellular functions and TEs, such as amino acids, isoprenoid biosynthesis, methyltransferase, ribosomes, group II intron bacterial retrotransposon, and transposase.

The functional importance of the differentially expressed genes in response to DENV infection across the three different time points potentially points toward a transcriptional response by *Wolbachia* to DENV infection and the associated cellular stress experienced. *Wolbachia* elicits the upregulation of RNase HI, an endoribonuclease capable of degrading RNA-DNA hybrids generated during viral replication in a non-sequence-specific manner, due to DENV infection at 1 hpi (64, 66, 67). This is followed by a stress response using the major DnaK/DnaJ chaperone system (*dnaJ* and *grpE* upregulated due to DENV infection at 1 hpi), which is used by prokaryotic symbionts in response to thermal stress (54, 78, 79), while concurrently upregulating genes associated with T1SS and T4SS transmembrane transport functions, known to facilitate the translocation of effector proteins such as ANKs involved in *Wolbachia*-host interactions (54, 94–97). Despite the upregulation of the major DnaK/DnaJ chaperone system and secretion pathway subunits at the very early stage of DENV infection, they were downregulated over time. Remarkably, the majority of DEGs at 6 hpi were downregulated, while 6S RNA, a ncRNA and known negative regulator of sigma 70-dependent gene transcription (98–102), was upregulated.

Unlike what we found in mosquito cells, a couple of studies on *Drosophila* did not find major transcriptional changes in *Wolbachia* following virus infection. In one study, the investigators combined a *Wolbachia*-infected *Drosophila melanogaster* cell line JW18 with the mosquito-borne Semliki Forest virus (SFV; alphavirus) to examine the mechanism of antiviral protection (51). RNA-Seq was performed on samples collected at 7 and 24 hpi; however, Rainey et al. reported a lack of differentially expressed *Wolbachia* genes between cells infected with and without SFV (51). Similarly, when *D. melanogaster* flies harboring the wMel2 strain of *Wolbachia* were infected with Sindbis virus (an alphavirus), no transcriptional changes in the wMel2 transcriptome were observed at 6, 24, and 48 h postinjection (106). The discrepancy between our findings and the two studies in *D. melanogaster* cell lines and flies could be due to differences in the *Wolbachia* strains, host cells, and the viruses used in the studies.

In conclusion, our findings shed new light on *Wolbachia*'s transcriptional response to DENV infection of the host cell and identify differentially expressed genes starting as early as 1 hpi, which to our knowledge, have not been examined so far. Further research, especially into RNase HI, 6S RNA, and other proteins and signaling molecules which are involved in *Wolbachia*'s response to stress and virus infection is necessary to uncover their potential contribution to antiviral protection. Furthermore, considering *Wolbachia* and cytoplasmic RNA viruses compete for resources, changes in the expression of genes that affect the availability of energy and resources to the virus, imposed by *Wolbachia*, could contribute to reduction in virus propagation. This line of research is, however, currently hampered due to the unavailability of tools to genetically modify or silence *Wolbachia* genes.

MATERIALS AND METHODS

Mosquito cell line maintenance. An Aag2.wAlbB cell line was developed previously (107) by transfecting Aag2 cells with wAlbB from Aa23 cells. Aa23 cells infected with wAlbB were established from eggs of *Aedes albopictus* (108). Cells were maintained in 1:1 Mitsuhashi-Maramorosch (Himedia) and Schneider's *Drosophila* medium (Invitrogen) supplemented with 10% fetal bovine serum (FBS; Bovogen Biologicals, France) at 27°C and passaged every 3 to 4 days.

Virus infection experiments. Prior to the infection of Aag2.wAlbB cells, *Wolbachia* density was quantified by quantitative PCR (qPCR). Genomic DNA was extracted from cells using the DIY spin column protocol as previously described (109). qPCR was performed using QuantiFast SYBR green PCR mix (Qiagen), in accordance with the manufacturer's instructions. Forward and reverse primers (wAlbB-*wsp*-qF and wAlbB-*wsp*-qR) (see Table S1 in the supplemental material) targeting the *Wolbachia* surface protein gene (*wsp*) and *A. aegypti* ribosomal protein subunit 17 gene (*RPS17*) (AeRPS17-qF and AeRPS17-qR) (Table S1) were used to amplify the target and the normalizing gene, respectively (14, 37). All qPCRs were performed in duplicates using a Rotor-Gene Q thermocycler (Qiagen) under the following conditions: 95°C for 5 min and then 40 cycles of 95°C for 10 s and combined annealing/extension at 60°C for 35 s. This was followed by a standard post-qPCR high-resolution melt analysis to assess the specificity of the amplified *wsp* and *RPS17* qPCR products. The relative abundance of *wsp* and *RPS17* was determined using the relative quantification method as described previously (110).

For virus infection, Aag2.wAlbB cells were seeded into 6-well culture plates (Greiner Bio-One) at 1.5×10^6 cells per well and allowed to adhere for 1 h at 27°C. Medium was then removed, and cells were

inoculated with DENV serotype 2 (DENV-2) East Timor strain (ET-300) at a multiplicity of infection (MOI) of 1. Uninfected cells were treated the same as Aag2.wAlbB virus-infected cells except without the addition of virus. All 6-well plates were incubated on a rocker for 1 h at room temperature followed by the removal of supernatant and subsequent replenishment with fresh medium. The plates were then incubated at 27°C. Aag2.wAlbB virus-infected and uninfected cells were collected at 1, 6, and 24 h postinfection (hpi) in three biological replicates for each time point. In our experimental design, we used matched time points for infected and uninfected samples to take into consideration possible changes of gene expression over time in both *Wolbachia* and host cells in cell culture. Cells were pelleted by centrifugation at $2,500 \times g$ for 3.5 min. Supernatant was discarded and pellets were frozen at -80°C for future RNA extraction.

Leftover RNA samples were used to confirm DENV-2 infection (see below for RNA extraction). For quantitation of DENV-2 genome copies in Aag2.wAlbB cells, first-strand cDNA synthesis was performed using M-MuLV reverse transcriptase (New England BioLabs) with a gene-specific (NS5) reverse primer (DENV2-qR) (Table S1) to amplify the DENV genomic RNA and *A. aegypti* RPS17 reverse primer (AeRPS17-qR) (Table S1) for the synthesis of the reference gene cDNA. In each RT reaction, 500 ng of DNase I-treated RNA was used as the template in a total volume of 20 μl . All the RT reactions were performed in a Veriti 96-well thermocycler (Applied Biosystems) under the following conditions: 65°C for 5 min, 50°C for 50 min, and 75°C for 15 min. For qPCR, the produced cDNA was diluted in a 1:5 ratio with Ultrapure DNase/RNase-free water (Invitrogen). Two microliters of the diluted cDNA was used for qPCRs with both forward and reverse gene-specific primers (DENV2-qF and DENV2-qR) (Table S1) used to amplify the DENV-2 NS5 region of the viral genome (111). *A. aegypti* RPS17 forward and reverse primers were used to amplify the normalizing gene (14). All qPCRs were performed in duplicates using a Rotor-Gene Q thermocycler (Qiagen) under the conditions specified above.

RNA extraction and sequencing. Total RNA from DENV-2-infected and uninfected Aag2.wAlbB cells was extracted using the Qiagen RNeasy minikit (Qiagen) according to the manufacturer's instructions. The obtained RNA pellets were resuspended in 30 μl of Ultrapure DNase/RNase-free water (Invitrogen) and treated with DNase I enzyme (TURBO DNase; Invitrogen) to remove genomic DNA from RNA samples as per the manufacturer's instructions. RNA sequencing (RNA-Seq) was conducted by GENEWIZ (GENEWIZ, China) under the following conditions. The RNA quality and quantity of each sample were assessed using a Bioanalyzer 2100 (Agilent Technologies), Agilent RNA 6000 Nano kit (Agilent Technologies), and 1% agarose gel. In total, 5 μg of total RNA per sample with an RNA integrity number of >7.0 was used for library preparation according to the manufacturer's protocol using NEBNext Ultra RNA library prep kit for Illumina (New England BioLabs). After removal of ribosomal RNAs using a Ribo-Zero-rRNA removal kit (Illumina), the mRNA fragmentation and priming were performed using NEBNext first-strand synthesis reaction buffer and NEBNext random primers (New England BioLabs). First-strand cDNA was synthesized using ProtoScript II reverse transcriptase, and the second-strand cDNA was synthesized using a second-strand synthesis enzyme mix (New England BioLabs). The double-stranded DNA was purified by AxyPrep Mag PCR clean-up (Axygen) and treated with End Prep enzyme mix to repair both ends and add deoxyribosyladenine (dA) tailing in one reaction, followed by a T-A ligation to add adaptors to both ends. Size selection of adaptor-ligated DNA was then performed using AxyPrep Mag PCR clean-up (Axygen), and fragments of ~ 360 bp (with the approximate insert size of 300 bp) were recovered. Each sample was then amplified by PCR using P5 and P7 primers (Table S1). The PCR products were cleaned up using AxyPrep Mag PCR clean-up (Axygen), validated using an Agilent 2100 Bioanalyzer (Agilent Technologies), and quantified by a Qubit 2.0 fluorometer (Invitrogen). Then, libraries with different indices were multiplexed and loaded on an Illumina HiSeq instrument according to the manufacturer's instructions (Illumina). Sequencing was carried out using a 2 by 150-bp paired-end (PE) configuration, and image analysis and base calling were conducted by the HiSeq Control Software (HCS)+OLB+GAPipeline-1.6 on the Illumina HiSeq instrument (Illumina). The sequences were processed and quality controlled by GENEWIZ.

Data quality control using demultiplexing was performed by bcl2fastq 2.17, and RNA-Seq raw data were filtered as follows. Low-quality pair-end reads with ambiguous nucleotide content of N bases of more than 10% and a ratio of bases of low quality (Phred quality score $Q < 20$) of more than 0.5 in either read were filtered out and discarded before data analysis. The paired-end raw reads were obtained as fastq files and then imported into CLC Genomics Workbench v20.0.2 (CLC-GWB; Qiagen) for further processing and analysis. The raw reads were trimmed from the 3' ends using the trim reads sequence tool in CLC-GWB in order to remove Illumina sequencing adapter P5 and P7. Default trim settings with automatic read-through adapter trimming and removal of low-quality sequences (Phred quality score = 0.05) were applied.

Differential gene expression analysis. Aag2.wAlbB high-quality trimmed paired-end reads were mapped to a combined reference genome assembly containing the *A. aegypti* strain LVP_AGWG AeagL5.0 chromosomes 1 to 3 (NC_035107, NC_035108, and NC_035109), mitochondrion complete genome (MF194022), *Wolbachia* wAlbB genome (CP031221), cell-fusing agent virus strain Galveston genome (CFAV; NC_001564), *Aedes albopictus* negev-like virus isolate (AaNLV; MK879802), and the *de novo* assembled DENV-2 ET-300 genome (see below for assembly). It was previously shown that Aag2.wAlbB cells are persistently infected with CFAV and AaNLV (112). The mapping setting "genome annotated with genes and transcripts suitable for Eukaryotes" was used, which accounts for splicing. Mapping parameters with a minimum length fraction of 0.8, minimum similarity fraction of 0.9, and maximum number of hits for a read of 30 to capture multimapping repetitive elements were applied. The CLC-GWB principal-component analysis (PCA) for RNA-Seq tool was used to create a two-dimensional principal component plot to identify outlying samples and variations in the sample data set.

The empirical analysis of differentially expressed genes (DEGs) was performed using the CLC-GWB differential expression for RNA-Seq tool with the default parameters to identify DEGs between DENV-infected and uninfected Aag2.wAlbB samples. TMM (trimmed mean of M values) normalization was used to calculate

effective library sizes as developed and described previously (113). The CLC-GWB differential expression for RNA-Seq tool uses multifactorial statistics based on a negative binomial generalized linear model (GLM) for this purpose (114). Differential gene expression in response to DENV infection was evaluated at 1, 6, and 24 hpi between virus-infected and uninfected samples, whereas the differential expression with respect to time and DENV infection was assessed between 1 versus 6, 6 versus 24, and 1 versus 24 hpi (Fig. S1). In the latter comparisons, up- or downregulation of a gene was considered over time. For both sets of analyses, we used CLC-GWB's "all group pairs" analysis, which tests for differences between all pairs of groups in a factor, including a Benjamini-Hochberg correction for multiple comparisons, and accordingly adjusts *P* values. Significance of DEGs was assessed using the Wald test, and results were then filtered based on a fold change of ≥ 2.0 , ≥ 1.5 , and adjusted *P* value of < 0.05 . The CLC-GWB create Venn diagram for RNA-Seq tool was used to compare and visualize the overlap of DEGs between the three sampling time points. Open reading frame (ORF) integrity of identified DEGs was assessed using the Swiss Institute of Bioinformatics (SIB) ExPasy protein analysis tool. A summary of the procedures from read mapping to the analysis of wAlbB differentially expressed genes in response to DENV infection is shown in Fig. S1.

For validation of DENV infection, normalized read counts mapping to the virus genome were used to estimate DENV abundance in each sample used for RNA-Seq.

De novo assembly of DENV-2 ET-300. After adapter and quality trimming of Aag2.wAlbB, clean reads were *de novo* assembled using CLC-GWB *de novo* assembly tool with the default parameters for word length, bubble, and minimum contig length of 200 nucleotides. Assembled contig reads were mapped back to contigs with stringent mapping settings (mismatch cost, 2; insertion cost, 3; deletion cost, 3; length fraction, 0.8; similarity fraction, 0.8) to eliminate false-positive mapping. CLC-GWB find ORFs tool with default settings was used to identify ORFs within the assembled contig. The assembled contig was then queried using NCBI's BLASTn (BLASTn v.2.10.1+) nonredundant nucleotide and BLASTp (BLASTp v.2.10.1+) nonredundant protein sequence databases.

Validation of DEGs using quantitative reverse transcription-PCR. For validation of the differentially expressed *Wolbachia* genes determined through RNA-Seq analysis, a total of 8 up- and downregulated genes were selected. The NCBI Primer-BLAST primer design tool was used to design primers for the selected DEGs and the 16S rRNA normalizing gene (115). The primers are listed in Table S1. New RNA samples were generated by repeating the infection experiment with DENV-2 ET-300 under identical conditions as before by collecting virus-infected and uninfected Aag2.wAlbB cells at 1, 6, and 24 hpi. RNA extraction, reverse transcription, and qPCR were performed as described above, except that first-strand cDNA synthesis was performed using SuperScript III reverse transcription (Invitrogen) and random hexamer primers (New England BioLabs) to synthesize a cDNA strand from extracted RNA as per the manufacturer's instructions. No reverse transcriptase control reactions were also included in the RT-qPCRs. *Wolbachia*'s 16S rRNA gene was used as the normalizing gene. The relative abundance of 16S rRNA and selected DEGs was determined using the relative quantification method as described previously (110).

Data availability. The RNA-Seq data generated in this study were submitted to SRA under the project ID [PRJNA669319](https://www.ncbi.nlm.nih.gov/sra/PRJNA669319).

SUPPLEMENTAL MATERIAL

Supplemental material is available online only.

FIG S1, TIF file, 0.2 MB.

FIG S2, TIF file, 0.1 MB.

FIG S3, TIF file, 0.1 MB.

TABLE S1, PDF file, 0.1 MB.

TABLE S2, XLSX file, 0.1 MB.

TABLE S3, XLSX file, 0.1 MB.

TABLE S4, XLSX file, 0.1 MB.

ACKNOWLEDGMENTS

Sassan Asgari is supported by the Australian Research Council (DP190102048). Cameron Bishop and Michael Leitner are supported by the University of Queensland Research Higher Degree scholarships.

We declare no conflict of interests.

REFERENCES

- Bhatt S, Gething P, Brady O, Messina J, Farlow A, Moyes C, Drake J, Brownstein J, Hoen A, Sankoh O, Myers M, George D, Jaenisch T, Wint G, Simmons C, Scott T, Farrar J, Hay S. 2013. The global distribution and burden of dengue. *Nature* 496:504–507. <https://doi.org/10.1038/nature12060>.
- Hill CA, Kafatos FC, Stansfield SK, Collins FH. 2005. Arthropod-borne diseases: vector control in the genomics era. *Nat Rev Microbiol* 3:262–268. <https://doi.org/10.1038/nrmicro1101>.
- Guzman MG, Halstead SB, Artsob H, Buchy P, Farrar J, Gubler DJ, Hunsperger E, Kroeger A, Margolis HS, Martinez E, Nathan MB, Pelegrino JL, Simmons C, Yoksan S, Peeling RW. 2010. Dengue: a continuing global threat. *Nat Rev Microbiol* 8:S7–S16. <https://doi.org/10.1038/nrmicro2460>.
- Acosta EG, Kumar A, Bartenschlager R. 2014. Revisiting dengue virus–host cell interaction: new insights into molecular and cellular virology. *Adv Virus Res* 88:1–109. <https://doi.org/10.1016/B978-0-12-800098-4.00001-5>.
- Kraemer MUG, Sinka ME, Duda KA, Mylne A, Shearer FM, Brady OJ, Messina JP, Barker CM, Moore CG, Carvalho RG, Coelho GE, Van Bortel W, Hendrickx G, Schaffner F, Wint GRW, Elyazar IRF, Teng H-J, Hay SI. 2015. The global compendium of *Aedes aegypti* and *A. albopictus* occurrence. *Sci Data* 2:150035. <https://doi.org/10.1038/sdata.2015.35>.

6. Liu-Helmersson J, Brännström Å, Sewe MO, Semenza JC, Rocklöv J. 2019. Estimating past, present, and future trends in the global distribution and abundance of the arbovirus vector *Aedes aegypti* under climate change scenarios. *Front Public Health* 7:148. <https://doi.org/10.3389/fpubh.2019.00148>.
7. Gubler DJ. 2011. Dengue, urbanization and globalization: the unholy trinity of the 21(st) century. *Trop Med Health* 39:3–11. <https://doi.org/10.2149/tmh.2011-S05>.
8. Gould E, Pettersson J, Higgs S, Charrel R, de Lamballerie X. 2017. Emerging arboviruses: why today? *One Health* 4:1–13. <https://doi.org/10.1016/j.onehlt.2017.06.001>.
9. Eder M, Cortes F, Teixeira de Siqueira Filha N, Araújo de França GV, Degroote S, Braga C, Ridde V, Turchi Martelli CM. 2018. Scoping review on vector-borne diseases in urban areas: transmission dynamics, vectorial capacity and co-infection. *Infect Dis Poverty* 7:90. <https://doi.org/10.1186/s40249-018-0475-7>.
10. Marcombe S, Mathieu RB, Pocquet N, Riaz M-A, Poupardin R, Sélior S, Darriet F, Reynaud S, Yébakima A, Corbel V, David J-P, Chandre F. 2012. Insecticide resistance in the dengue vector *Aedes aegypti* from Martinique: distribution, mechanisms and relations with environmental factors. *PLoS One* 7:e30989. <https://doi.org/10.1371/journal.pone.0030989>.
11. Marcombe S, Carron A, Darriet F, Etienne M, Agnew P, Tolosa M, Yp-Tcha MM, Lagneau C, Yébakima A, Corbel V. 2009. Reduced efficacy of pyrethroid space sprays for dengue control in an area of Martinique with pyrethroid resistance. *Am J Trop Med Hygiene* 80:745–751. <https://doi.org/10.4269/ajtmh.2009.80.745>.
12. Bellinato DF, Viana-Medeiros PF, Araujo SC, Martins AJ, Lima JB, Valle D. 2016. Resistance status to the insecticides temephos, deltamethrin, and diflubenzuron in Brazilian *Aedes aegypti* populations. *BioMed Res Int* 2016:8603263. <https://doi.org/10.1155/2016/8603263>.
13. Moyes C, Vontas J, Martins A, Ng LC, Kooou S, Dufour I, Raghavendra K, Pinto J, Corbel V, David JP, Weetman D. 2017. Contemporary status of insecticide resistance in the major *Aedes* vectors of arboviruses infecting humans. *PLoS Negl Trop Dis* 11:e0005625. <https://doi.org/10.1371/journal.pntd.0005625>.
14. Moreira LA, Iturbe-Ormaetxe I, Jeffery JA, Lu G, Pyke AT, Hedges LM, Rocha BC, Hall-Mendelin S, Day A, Riegler M, Hugo LE, Johnson KN, Kay BH, McGraw EA, van Den Hurk AF, Ryan PA, O'Neill SL. 2009. A *Wolbachia* symbiont in *Aedes aegypti* limits infection with dengue, chikungunya, and *Plasmodium*. *Cell* 139:1268–1278. <https://doi.org/10.1016/j.cell.2009.11.042>.
15. Bian G, Xu Y, Lu P, Xie Y, Xi Z. 2010. The endosymbiotic bacterium *Wolbachia* induces resistance to dengue virus in *Aedes aegypti* (*Wolbachia*-dengue interactions). *PLoS Pathog* 6:e1000833. <https://doi.org/10.1371/journal.ppat.1000833>.
16. Walker T, Johnson PH, Moreira LA, Iturbe-Ormaetxe I, Frentiu FD, McMeniman CJ, Leong YS, Dong Y, Axford J, Kriesner P, Lloyd AL, Ritchie SA, O'Neill SL, Hoffmann AA. 2011. The wMel *Wolbachia* strain blocks dengue and invades caged *Aedes aegypti* populations. *Nature* 476:450–453. <https://doi.org/10.1038/nature10355>.
17. Rasgon JL, Gamston CE, Ren X. 2006. Survival of *Wolbachia pipientis* in cell-free medium. *Appl Environ Microbiol* 72:6934–6937. <https://doi.org/10.1128/AEM.01673-06>.
18. Zug R, Hammerstein P. 2012. Still a host of hosts for *Wolbachia*: analysis of recent data suggests that 40% of terrestrial arthropod species are infected. *PLoS One* 7:e38544. <https://doi.org/10.1371/journal.pone.0038544>.
19. de Oliveira CD, Gonçalves DS, Baton LA, Shimabukuro PHF, Carvalho FD, Moreira LA. 2015. Broader prevalence of *Wolbachia* in insects including potential human disease vectors. *Bull Entomol Res* 105:305–315. <https://doi.org/10.1017/S0007485315000085>.
20. Dobson SL, Marsland EJ, Rattanadechakul W. 2002. Mutualistic *Wolbachia* infection in *Aedes albopictus*: accelerating cytoplasmic drive. *Genetics* 160:1087–1094. <https://doi.org/10.1093/genetics/160.3.1087>.
21. McGraw EA, O'Neill SL. 2004. *Wolbachia pipientis*: intracellular infection and pathogenesis in *Drosophila*. *Curr Opin Microbiol* 7:67–70. <https://doi.org/10.1016/j.mib.2003.12.003>.
22. Werren JH, Baldo L, Clark ME. 2008. *Wolbachia*: master manipulators of invertebrate biology. *Nat Rev Microbiol* 6:741–751. <https://doi.org/10.1038/nrmicro1969>.
23. Weeks AR, Turelli M, Harcombe WR, Reynolds KT, Hoffmann AA. 2007. From parasite to mutualist: rapid evolution of *Wolbachia* in natural populations of *Drosophila*. *PLoS Biol* 5:e114. <https://doi.org/10.1371/journal.pbio.0050114>.
24. Jiggins FM. 2017. The spread of *Wolbachia* through mosquito populations. *PLoS Biol* 15:e2002780. <https://doi.org/10.1371/journal.pbio.2002780>.
25. Hedges LM, Brownlie JC, O'Neill SL, Johnson KN. 2008. *Wolbachia* and virus protection in insects. *Science* 322:702. <https://doi.org/10.1126/science.1162418>.
26. Teixeira L, Ferreira A, Ashburner M. 2008. The bacterial symbiont *Wolbachia* induces resistance to RNA viral infections in *Drosophila melanogaster*. *PLoS Biol* 6:e1000002. <https://doi.org/10.1371/journal.pbio.1000002>.
27. McMeniman CJ, Lane RV, Cass BN, Fong AW, Sidhu M, Wang YF, O'Neill SL. 2009. Stable introduction of a life-shortening *Wolbachia* infection into the mosquito *Aedes aegypti*. *Science* 323:141–144. <https://doi.org/10.1126/science.1165326>.
28. Kambris Z, Cook PE, Phuc HK, Sinkins SP. 2009. Immune activation by life-shortening *Wolbachia* and reduced filarial competence in mosquitoes. *Science* 326:134–136. <https://doi.org/10.1126/science.1177531>.
29. Rancès E, Ye YH, Woolfit M, McGraw EA, O'Neill SL. 2012. The relative importance of innate immune priming in *Wolbachia*-mediated dengue interference. *PLoS Pathog* 8:e1002548. <https://doi.org/10.1371/journal.ppat.1002548>.
30. Terradas G, McGraw EA. 2017. *Wolbachia*-mediated virus blocking in the mosquito vector *Aedes aegypti*. *Curr Opin Insect Sci* 22:37–44. <https://doi.org/10.1016/j.cois.2017.05.005>.
31. McFarlane M, Arias-Goeta C, Martin E, O'Hara Z, Lulla A, Mousson L, Rainey SM, Misbah S, Schnettler E, Donald CL, Merits A, Kohl A, Failloux A-B. 2014. Characterization of *Aedes aegypti* innate-immune pathways that limit chikungunya virus replication. *PLoS Negl Trop Dis* 8:e2994. <https://doi.org/10.1371/journal.pntd.0002994>.
32. Sanchez-Vargas I, Scott JC, Poole-Smith BK, Franz AW, Barbosa-Solomieu V, Wilusz J, Olson KE, Blair CD. 2009. Dengue virus type 2 infections of *Aedes aegypti* are modulated by the mosquito's RNA interference pathway. *PLoS Pathog* 5:e1000299. <https://doi.org/10.1371/journal.ppat.1000299>.
33. Fragkoudis R, Attarzadeh-Yazdi G, Nash AA, Fazakerley JK, Kohl A. 2009. Advances in dissecting mosquito innate immune responses to arbovirus infection. *J Gen Virol* 90:2061–2072. <https://doi.org/10.1099/vir.0.013201-0>.
34. Blair CD. 2011. Mosquito RNAi is the major innate immune pathway controlling arbovirus infection and transmission. *Future Microbiol* 6:265–277. <https://doi.org/10.2217/fmb.11.11>.
35. Sim S, Jupatanakul N, Dimopoulos G. 2014. Mosquito immunity against arboviruses. *Viruses* 6:4479–4504. <https://doi.org/10.3390/v6114479>.
36. Hussain M, Etebari K, Asgari S. 2016. Functions of small RNAs in mosquitoes. *Adv Insect Physiol* 51:189–222. <https://doi.org/10.1016/bs.aip.2016.04.001>.
37. Hussain M, Frentiu FD, Moreira LA, O'Neill SL, Asgari S. 2011. *Wolbachia* uses host microRNAs to manipulate host gene expression and facilitate colonization of the dengue vector *Aedes aegypti*. *Proc Natl Acad Sci U S A* 108:9250–9255. <https://doi.org/10.1073/pnas.1105469108>.
38. Terradas G, Joubert DA, McGraw EA. 2017. The RNAi pathway plays a small part in *Wolbachia*-mediated blocking of dengue virus in mosquito cells. *Sci Rep* 7:43847. <https://doi.org/10.1038/srep43847>.
39. Campbell CL, Keene KM, Brackney DE, Olson KE, Blair CD, Wilusz J, Foy BD. 2008. *Aedes aegypti* uses RNA interference in defense against Sindbis virus infection. *BMC Microbiol* 8:47. <https://doi.org/10.1186/1471-2180-8-47>.
40. Hedges LM, Yamada R, O'Neill SL, Johnson KN. 2012. The small interfering RNA pathway is not essential for *Wolbachia*-mediated antiviral protection in *Drosophila melanogaster*. *Appl Environ Microbiol* 78:6773–6776. <https://doi.org/10.1128/AEM.01650-12>.
41. Caragata EP, Rances E, O'Neill SL, McGraw EA. 2014. Competition for amino acids between *Wolbachia* and the mosquito host, *Aedes aegypti*. *Microb Ecol* 67:205–218. <https://doi.org/10.1007/s00248-013-0339-4>.
42. Ziegler R, Ibrahim MM. 2001. Formation of lipid reserves in fat body and eggs of the yellow fever mosquito, *Aedes aegypti*. *J Insect Physiol* 47:623–627. [https://doi.org/10.1016/s0022-1910\(00\)00158-x](https://doi.org/10.1016/s0022-1910(00)00158-x).
43. Lindsey A, Bhattacharya T, Newton I, Hardy RW. 2018. Conflict in the intracellular lives of endosymbionts and viruses: a mechanistic look at *Wolbachia*-mediated pathogen-blocking. *Viruses* 10:141. <https://doi.org/10.3390/v10040141>.
44. Johnson K. 2015. The impact of *Wolbachia* on virus infection in mosquitoes. *Viruses* 7:5705–5717. <https://doi.org/10.3390/v7112903>.
45. Terradas G, Allen SL, Chenoweth SF, McGraw EA. 2017. Family level variation in *Wolbachia*-mediated dengue virus blocking in *Aedes aegypti*. *Parasit Vectors* 10:622. <https://doi.org/10.1186/s13071-017-2589-3>.
46. Lu P, Bian G, Pan X, Xi Z. 2012. *Wolbachia* induces density-dependent inhibition to dengue virus in mosquito cells. *PLoS Negl Trop Dis* 6:e1754. <https://doi.org/10.1371/journal.pntd.0001754>.
47. Mousson L, Zouache K, Arias-Goeta C, Raquin V, Mavingui P, Failloux A-B. 2012. The native *Wolbachia* symbionts limit transmission of dengue virus

- in *Aedes albopictus*. *PLoS Negl Trop Dis* 6:e1989. <https://doi.org/10.1371/journal.pntd.0001989>.
48. Bian G, Zhou G, Lu P, Xi Z. 2013. Replacing a native *Wolbachia* with a novel strain results in an increase in endosymbiont load and resistance to dengue virus in a mosquito vector. *PLoS Negl Trop Dis* 7:e2250. <https://doi.org/10.1371/journal.pntd.0002250>.
 49. Chouin-Carneiro T, Ant TH, Herd C, Louis F, Failloux AB, Sinkins SP. 2020. *Wolbachia* strain wAlbA blocks Zika virus transmission in *Aedes aegypti*. *Med Vet Entomol* 34:116–119. <https://doi.org/10.1111/mve.12384>.
 50. Fraser JE, O'Donnell TB, Duyvestyn JM, O'Neill SL, Simmons CP, Flores HA. 2020. Novel phenotype of *Wolbachia* strain wPip in *Aedes aegypti* challenges assumptions on mechanisms of *Wolbachia*-mediated dengue virus inhibition. *PLoS Pathog* 16:e1008410. <https://doi.org/10.1371/journal.ppat.1008410>.
 51. Rainey SM, Martinez J, McFarlane M, Juneja P, Sarkies P, Lulla A, Schnettler E, Varjak M, Merits A, Miska EA, Jiggins FM, Kohl A. 2016. *Wolbachia* blocks viral genome replication early in infection without a transcriptional response by the endosymbiont or host small RNA pathways. *PLoS Pathog* 12:e1005536. <https://doi.org/10.1371/journal.ppat.1005536>.
 52. Bhattacharya T, Newton ILG, Hardy RW. 2020. Viral RNA is a target for *Wolbachia*-mediated pathogen blocking. *PLoS Pathog* 16:e1008513. <https://doi.org/10.1371/journal.ppat.1008513>.
 53. Sakoonwatanyoo P, Boonsanay V, Smith DR. 2006. Growth and production of the dengue virus in C6/36 cells and identification of a laminin-binding protein as a candidate serotype 3 and 4 receptor protein. *Inter-virology* 49:161–172. <https://doi.org/10.1159/000089377>.
 54. Sinha A, Li Z, Sun L, Carlow CKS. 2019. Complete genome sequence of the *Wolbachia* wAlbB endosymbiont of *Aedes albopictus*. *Genome Biol Evol* 11:706–720. <https://doi.org/10.1093/gbe/evz025>.
 55. Matthews BJ, Dudchenko O, Kingan SB, Koren S, Antoshechkin I, Crawford JE, Glassford WJ, Herre M, Redmond SN, Rose NH, Weedall GD, Wu Y, Batra SS, Brito-Sierra CA, Buckingham SD, Campbell CL, Chan S, Cox E, Evans BR, Fansiri T, Filipović I, Fontaine A, Gloria-Soria A, Hall R, Joardar VS, Jones AK, Kay RGG, Kodali VK, Lee J, Lycett GJ, Mitchell SN, Muehling J, Murphy MR, Omer AD, Partridge FA, Peluso P, Aiden AP, Ramasamy V, Rašić G, Roy S, Saavedra-Rodriguez K, Sharan S, Sharma A, Smith ML, Turner J, Weakley AM, Zhao Z, Akbari OS, Black WC, IV, Cao H, et al. 2018. Improved reference genome of *Aedes aegypti* informs arbovirus vector control. *Nature* 563:501–507. <https://doi.org/10.1038/s41586-018-0692-z>.
 56. Etebari K, Hegde S, Saldaña MA, Widen SG, Wood TG, Asgari S, Hughes GL. 2017. Global transcriptome analysis of *Aedes aegypti* mosquitoes in response to Zika virus infection. *mSphere* 2:e00456-17. <https://doi.org/10.1128/mSphere.00456-17>.
 57. Woolfit M, Algama M, Keith JM, McGraw EA, Popovici J. 2015. Discovery of putative small non-coding RNAs from the obligate intracellular bacterium *Wolbachia pipientis*. *PLoS One* 10:e0118595. <https://doi.org/10.1371/journal.pone.0118595>.
 58. Chambers TJ, Hahn CS, Galler R, Rice CM. 1990. Flavivirus genome organization, expression, and replication. *Annu Rev Microbiol* 44:649–688. <https://doi.org/10.1146/annurev.mi.44.100190.003245>.
 59. Gebhard LG, Filomatori CV, Gamarnik AV. 2011. Functional RNA elements in the dengue virus genome. *Viruses* 3:1739–1756. <https://doi.org/10.3390/v3091739>.
 60. Dwivedi VD, Tripathi IP, Tripathi RC, Bharadwaj S, Mishra SK. 2017. Genomics, proteomics and evolution of dengue virus. *Brief Funct Genomics* 16:217–227. <https://doi.org/10.1093/bfpg/elw040>.
 61. Hussain M, Lu G, Torres S, Edmonds JH, Kay BH, Khromykh AA, Asgari S. 2013. Effect of *Wolbachia* on replication of West Nile virus in a mosquito cell line and adult mosquitoes. *J Virol* 87:851–858. <https://doi.org/10.1128/JVI.01837-12>.
 62. Colpitts TM, Cox J, Vanlandingham DL, Feitosa FM, Cheng G, Kurscheid S, Wang P, Krishnan MN, Higgs S, Fikrig E. 2011. Alterations in the *Aedes aegypti* transcriptome during infection with West Nile, dengue and yellow fever viruses. *PLoS Pathog* 7:e1002189. <https://doi.org/10.1371/journal.ppat.1002189>.
 63. Bonizzoni M, Dunn WA, Campbell CL, Olson KE, Marinotti O, James AA. 2012. Complex modulation of the *Aedes aegypti* transcriptome in response to dengue virus infection. *PLoS One* 7:e50512. <https://doi.org/10.1371/journal.pone.0050512>.
 64. Cerritelli SM, Crouch RJ. 2009. Ribonuclease H: the enzymes in eukaryotes. *FEBS J* 276:1494–1505. <https://doi.org/10.1111/j.1742-4658.2009.06908.x>.
 65. Majorek KA, Dunin-Horkawicz S, Steczkiewicz K, Muszewska A, Nowotny M, Ginalski K, Bujnicki JM. 2014. The RNase H-like superfamily: new members, comparative structural analysis and evolutionary classification. *Nucleic Acids Res* 42:4160–4179. <https://doi.org/10.1093/nar/gkt1414>.
 66. Tannous E, Kanaya E, Kanaya S. 2015. Role of RNase H1 in DNA repair: removal of single ribonucleotide misincorporated into DNA in collaboration with RNase H2. *Sci Rep* 5:9969. <https://doi.org/10.1038/srep09969>.
 67. Hartmann G. 2017. Nucleic acid immunity. *Adv Immunol* 133:121–169. <https://doi.org/10.1016/bs.ai.2016.11.001>.
 68. Anupama K, Leela JK, Gowrishankar J. 2011. Two pathways for RNase E action in *Escherichia coli* in vivo and bypass of its essentiality in mutants defective for Rho-dependent transcription termination. *Mol Microbiol* 82:1330–1348. <https://doi.org/10.1111/j.1365-2958.2011.07895.x>.
 69. Koonin EV. 2017. Evolution of RNA- and DNA-guided antiviral defense systems in prokaryotes and eukaryotes: common ancestry vs convergence. *Biol Direct* 12:5. <https://doi.org/10.1186/s13062-017-0177-2>.
 70. Laalami S, Zig L, Putzer H. 2014. Initiation of mRNA decay in bacteria. *Cell Mol Life Sci* 71:1799–1828. <https://doi.org/10.1007/s00018-013-1472-4>.
 71. Moelling K, Broecker F, Russo G, Sunagawa S. 2017. RNase H as gene modifier, driver of evolution and antiviral defense. *Front Microbiol* 8:1745. <https://doi.org/10.3389/fmicb.2017.01745>.
 72. Fukui K, Kuramitsu S. 2011. Structure and function of the small MutS-related domain. *Mol Biol Int* 2011:691735. <https://doi.org/10.4061/2011/691735>.
 73. Qiu R, Sakato M, Sacho EJ, Wilkins H, Zhang X, Modrich P, Hingorani MM, Erie DA, Weninger KR. 2015. MutL traps MutS at a DNA mismatch. *Proc Natl Acad Sci U S A* 112:10914–10919. <https://doi.org/10.1073/pnas.1505655112>.
 74. Delaney JM. 1990. A *grpE* mutant of *Escherichia coli* is more resistant to heat than the wild-type. *J Gen Microbiol* 136:797–801. <https://doi.org/10.1099/00221287-136-5-797>.
 75. Harrison CJ, Hayer-Hartl M, Di Liberto M, Hartl F, Kuriyan J. 1997. Crystal structure of the nucleotide exchange factor GrpE bound to the ATPase domain of the molecular chaperone DnaK. *Science* 276:431–435. <https://doi.org/10.1126/science.276.5311.431>.
 76. Harrison C. 2003. GrpE, a nucleotide exchange factor for DnaK. *Cell Stress Chaperones* 8:218–224. [https://doi.org/10.1379/1466-1268\(2003\)008<0218:GANEFF>2.0.CO;2](https://doi.org/10.1379/1466-1268(2003)008<0218:GANEFF>2.0.CO;2).
 77. Aguilar-Rodríguez J, Sabater-Muñoz B, Montagud-Martínez R, Berlanga V, Alvarez-Ponce D, Wagner A, Fares MA. 2016. The molecular chaperone DnaK is a source of mutational robustness. *Genome Biol Evol* 8:2979–2991. <https://doi.org/10.1093/gbe/evw176>.
 78. Roma JS, D'Souza S, Somers PJ, Cabo LF, Farsin R, Aksoy S, Runyen-Janecky LJ, Weiss BL. 2019. Thermal stress responses of *Sodalis glossinidius*, an indigenous bacterial symbiont of hematophagous tsetse flies. *PLoS Negl Trop Dis* 13:e0007464. <https://doi.org/10.1371/journal.pntd.0007464>.
 79. Bhandari V, Houry WA. 2015. Substrate interaction networks of the *Escherichia coli* chaperones: trigger factor, DnaK and GroEL. *Adv Exp Med Biol* 883:271–294. https://doi.org/10.1007/978-3-319-23603-2_15.
 80. Ren Q, Paulsen IT. 2005. Comparative analyses of fundamental differences in membrane transport capabilities in prokaryotes and eukaryotes. *PLoS Comput Biol* 1:e27. <https://doi.org/10.1371/journal.pcbi.0010027>.
 81. Atkins HS, Dassa E, Walker NJ, Griffin KF, Harland DN, Taylor RR, Duffield ML, Titball RW. 2006. The identification and evaluation of ATP binding cassette systems in the intracellular bacterium *Francisella tularensis*. *Res Microbiol* 157:593–604. <https://doi.org/10.1016/j.resmic.2005.12.004>.
 82. Davidson AL, Dassa E, Orelle C, Chen J. 2008. Structure, function, and evolution of bacterial ATP-binding cassette systems. *Microbiol Mol Biol Rev* 72:317–364. <https://doi.org/10.1128/MMBR.00031-07>.
 83. Lindsey ARI. 2020. Sensing, signaling, and secretion: a review and analysis of systems for regulating host interaction in *Wolbachia*. *Genes* 11:813. <https://doi.org/10.3390/genes11070813>.
 84. Bing XL, Zhao DS, Sun JT, Zhang KJ, Hong XY. 2020. Genomic analysis of *Wolbachia* from *Laodelphax striatellus* (Delphacidae, Hemiptera) reveals insights into its "Jekyll and Hyde" mode of infection pattern. *Genome Biol Evol* 12:3818–3831. <https://doi.org/10.1093/gbe/evaa006>.
 85. Kanonenberg K, Spitz O, Erenburg IN, Beer T, Schmitt L. 2018. Type I secretion system-it takes three and a substrate. *FEMS Microbiol Lett* 365:fnv094. <https://doi.org/10.1093/femsle/fny094>.
 86. Gillespie JJ, Ammerman NC, Dreher-Lesnicks SM, Rahman MS, Worley MJ, Setubal JC, Sobral BS, Azad AF. 2009. An anomalous type IV secretion system in *Rickettsia* is evolutionarily conserved. *PLoS One* 4:e4833. <https://doi.org/10.1371/journal.pone.0004833>.

87. Grohmann E, Christie PJ, Waksman G, Backert S. 2018. Type IV secretion in Gram-negative and Gram-positive bacteria. *Mol Microbiol* 107:455–471. <https://doi.org/10.1111/mmi.13896>.
88. Bhattacharya T, Newton ILG. 2019. Mi casa es su casa: how an intracellular symbiont manipulates host biology. *Environ Microbiol* 21:3188–3196. <https://doi.org/10.1111/1462-2920.13964>.
89. Gillespie JJ, Phan IQH, Scheib H, Subramanian S, Edwards TE, Lehman SS, Piitulainen H, Rahman MS, Rennoll-Bankert KE, Staker BL, Taira S, Stacy R, Myler PJ, Azad AF, Pulliainen AT. 2015. Structural insight into how bacteria prevent interference between multiple divergent type IV secretion systems. *mBio* 6:e01867-15. <https://doi.org/10.1128/mBio.01867-15>.
90. Henderson KL, Felth LC, Molzahn CM, Shkel I, Wang S, Chhabra M, Ruff EF, Bieter L, Kraft JE, Record MT, Jr. 2017. Mechanism of transcription initiation and promoter escape by *E. coli* RNA polymerase. *Proc Natl Acad Sci U S A* 114:E3032–E3040. <https://doi.org/10.1073/pnas.1618675114>.
91. Lee J, Borukhov S. 2016. Bacterial RNA polymerase-DNA interaction—the driving force of gene expression and the target for drug action. *Front Mol Biosci* 3:73. <https://doi.org/10.3389/fmolb.2016.00073>.
92. Sutherland C, Murakami KS. 2018. An introduction to the structure and function of the catalytic core enzyme of *Escherichia coli* RNA polymerase. *EcoSal Plus* 8:ESP-0004-2018. <https://doi.org/10.1128/ecosalplus.ESP-0004-2018>.
93. Kent BN, Bordenstein SR. 2010. Phage WO of *Wolbachia*: lambda of the endosymbiont world. *Trends Microbiol* 18:173–181. <https://doi.org/10.1016/j.tim.2009.12.011>.
94. Bordenstein SR, Bordenstein SR. 2016. Eukaryotic association module in phage WO genomes from *Wolbachia*. *Nat Commun* 7:13155. <https://doi.org/10.1038/ncomms13155>.
95. Iturbe-Ormaetxe I, Burke GR, Riegler M, Neill SL. 2005. Distribution, expression, and motif variability of ankyrin domain genes in *Wolbachia pipientis*. *J Bacteriol* 187:5136–5145. <https://doi.org/10.1128/JB.187.15.5136-5145.2005>.
96. Siozios S, Ioannidis P, Klasson L, Andersson SGE, Braig HR, Bourtzis K. 2013. The diversity and evolution of *Wolbachia* ankyrin repeat domain genes. *PLoS One* 8:e55390. <https://doi.org/10.1371/journal.pone.0055390>.
97. Walker T, Klasson L, Sebahia M, Sanders MJ, Thomson NR, Parkhill J, Sinkins SP. 2007. Ankyrin repeat domain-encoding genes in the wPip strain of *Wolbachia* from the *Culex pipiens* group. *BMC Biol* 5:39. <https://doi.org/10.1186/1741-7007-5-39>.
98. Cavanagh AT, Klocko AD, Liu X, Wassarman KM. 2008. Promoter specificity for 6S RNA regulation of transcription is determined by core promoter sequences and competition for region 4.2 of sigma70. *Mol Microbiol* 67:1242–1256. <https://doi.org/10.1111/j.1365-2958.2008.06117.x>.
99. Schlüter JP, Reinkensmeier J, Barnett MJ, Lang C, Krol E, Giegerich R, Long SR, Becker A. 2013. Global mapping of transcription start sites and promoter motifs in the symbiotic α -proteobacterium *Sinorhizobium meliloti* 1021. *BMC Genomics* 14:156. <https://doi.org/10.1186/1471-2164-14-156>.
100. Trotochaud AE, Wassarman KM. 2005. A highly conserved 6S RNA structure is required for regulation of transcription. *Nat Struct Mol Biol* 12:313–319. <https://doi.org/10.1038/nsmb917>.
101. Wassarman KM, Storz G. 2000. 6S RNA regulates *E. coli* RNA polymerase activity. *Cell* 101:613–623. [https://doi.org/10.1016/s0092-8674\(00\)80873-9](https://doi.org/10.1016/s0092-8674(00)80873-9).
102. Weinberg Z, Wang JX, Bogue J, Yang J, Corbino K, Moy RH, Breaker RR. 2010. Comparative genomics reveals 104 candidate structured RNAs from bacteria, archaea, and their metagenomes. *Genome Biol* 11:R31. <https://doi.org/10.1186/gb-2010-11-3-r31>.
103. Mayoral JG, Hussain M, Joubert DA, Iturbe-Ormaetxe I, O'Neill SL, Asgari S. 2014. *Wolbachia* small noncoding RNAs and their role in cross-kingdom communications. *Proc Natl Acad Sci U S A* 111:18721–18726. <https://doi.org/10.1073/pnas.1420131112>.
104. Fan C, Wu YH, Decker CM, Rohani R, Gesell Salazar M, Ye H, Cui Z, Schmidt F, Huang WE. 2019. Defensive function of transposable elements in bacteria. *ACS Synth Biol* 8:2141–2151. <https://doi.org/10.1021/acssynbio.9b00218>.
105. Vigil-Stenman T, Ininbergs K, Bergman B, Ekman M. 2017. High abundance and expression of transposases in bacteria from the Baltic Sea. *ISME J* 11:2611–2623. <https://doi.org/10.1038/ismej.2017.114>.
106. Lindsey ARI, Bhattacharya T, Newton I, Hardy RW. 2021. *Wolbachia* and virus alter the host transcriptome at the interface of nucleotide metabolism pathways. *mBio* 12:e03472-20. <https://doi.org/10.1128/mBio.03472-20>.
107. Parry R, Bishop C, De Hayr L, Asgari S. 2019. Density-dependent enhanced replication of a dengue virus in *Wolbachia*-infected *Aedes* cells is associated with production of piRNAs and higher virus-derived siRNAs. *Virology* 528:89–100. <https://doi.org/10.1016/j.virol.2018.12.006>.
108. O'Neill SL, Pettigrew MM, Sinkins SP, Braig HR, Andreadis TG, Tesh RB. 1997. *In vitro* cultivation of *Wolbachia pipientis* in an *Aedes albopictus* cell line. *Insect Mol Biol* 6:33–39. <https://doi.org/10.1046/j.1365-2583.1997.00157.x>.
109. Ridley AW, Hereward JP, Daghli GJ, Raghu S, McCulloch GA, Walter GH. 2016. Flight of *Rhyzopertha dominica* (Coleoptera: Bostrichidae)—a spatio-temporal analysis with pheromone trapping and population genetics. *J Econ Entomol* 109:2561–2571. <https://doi.org/10.1093/jee/tow226>.
110. Pfaffl MW, Horgan GW, Dempfle L. 2002. Relative expression software tool (REST) for group-wise comparison and statistical analysis of relative expression results in real-time PCR. *Nucleic Acids Res* 30:e36. <https://doi.org/10.1093/nar/30.9.e36>.
111. Asad S, Hussain M, Hugo L, Osei-Amo S, Zhang G, Watterson D, Asgari S. 2018. Suppression of the pelo protein by *Wolbachia* and its effect on dengue virus in *Aedes aegypti*. *PLoS Negl Trop Dis* 12:e0006405. <https://doi.org/10.1371/journal.pntd.0006405>.
112. Bishop C, Parry R, Asgari S. 2020. Effect of *Wolbachia* wAlbB on a positive-sense RNA negev-like virus: a novel virus persistently infecting *Aedes albopictus* mosquitoes and cells. *J Gen Virol* 101:216–225. <https://doi.org/10.1099/jgv.0.001361>.
113. Robinson MD, Oshlack A. 2010. A scaling normalization method for differential expression analysis of RNA-seq data. *Genome Biol* 11:R25. <https://doi.org/10.1186/gb-2010-11-3-r25>.
114. McCarthy DJ, Chen Y, Smyth GK. 2012. Differential expression analysis of multifactor RNA-Seq experiments with respect to biological variation. *Nucleic Acids Res* 40:4288–4297. <https://doi.org/10.1093/nar/gks042>.
115. Ye J, Coulouris G, Zaretskaya I, Cutcutache I, Rozen S, Madden TL. 2012. Primer-BLAST: a tool to design target-specific primers for polymerase chain reaction. *BMC Bioinformatics* 13:134. <https://doi.org/10.1186/1471-2105-13-134>.